Enhanced Pool Scrubber Code Significantly Improves Decontamination Factor Projections

Hyeon Ho Byun, Man Sung Yim*
Department of Nuclear and Quantum Engineering, Korea Advanced Institute of Science and Technology, 291 Daehakro, Yuseong-gu, Daejeon 34141, Republic of Korea
**Corresponding author: Tel) 82-42-350-3836*
E-mail address) msyim@kaist.ac.kr

1. Introduction

Governments such as Finland and South Korea have adopted a stricter safety design criterion of nuclear power plant (NPP). This newly adopted criterion requires radioactive release lower than 100TBq during severe accident. Currently, some NPPs implemented containment filtered venting system (CFVS) for the mitigation of cesium 137 release under severe accident condition. Pool scrubber (PS) has an important role for filtration of gaseous iodine and radioactive aerosols.

A PS is relatively simple water based filtration system (see Fig. 1). Radioactive releases are directed into the bottom of a water tank, and injected into the water through nozzles. While nozzles convert the gas to bubbles containing radioactive aerosols, deposition mechanisms work at the bubble surface. Deposited radioactive aerosols are accumulated in the water, and filtrated gas is released into the environment.

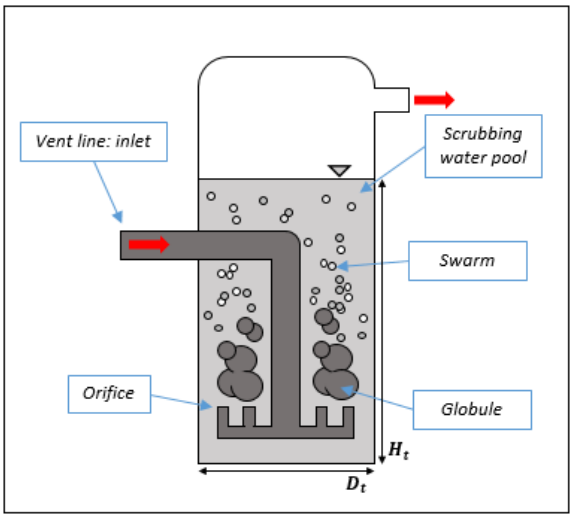

Fig. 1. PS scheme

In order to evaluate the overall filtration efficiency of PS, some experimental studies have been carried out in 1980~1990s. However, PS experiment requires very high cost setup, simulation codes are alternatively developed to assess the filtration efficiency of PS. Historically, BUSCA and SPARC are the most commonly used for PS assessment. However, it is accepted that they do not accurately predict the decontamination factors (DFs) of PS, because they used too simplified bubble population models and inaccurate hydrodynamic models. Consequently, DFs obtained by BUSCA and SPARC are generally more conservative than experimentally obtained DFs under the same condition.

To avoid these conservatism, the main task of this study is to develop a code that improved the DF projections for a PS. Some fundamental concepts are based on BUSCA and SPARC codes, and some specific improvements such as bubble breakup and pool hydrodynamics are newly involved. This study firstly explains the skeletons of improved PS code, and module details are described. At last, we will compare DFs driven by our improved PS code (SPS) with respect to the experimental DFs and other PS codes (BUSCA and SPARC).

2. Methods and Results

Existing PS codes conceptually involve bubble formation, bubble breakup, and deposition velocity modules (see Fig. 2).

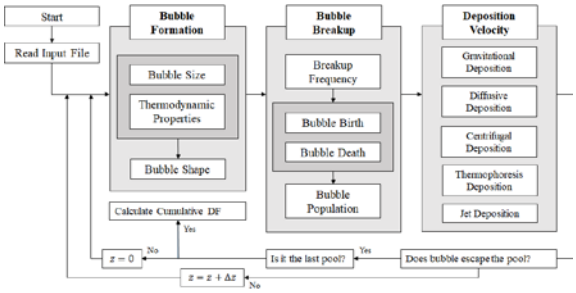

Fig. 2. General PS code skeleton

DF is a main parameter determining filtration efficiency of PS. Existing codes calculate the DF based on the single representative bubble. However, one of the important reason of DF conservatisms of existing codes (BUSCA and SPARC) is neglect of aerosol depositions from the other size bubbles. Hence SPS defines pool DF as follows:

$$\mathrm{DF} = \prod_k \frac{\sum_j \sum_i m_{p,ijk} \cdot N_{b,jk}}{\sum_j \sum_i m_{p,ijk} \cdot N_{b,jk} \cdot \left(1 - \mathrm{Eff}_{ijk}\right)} \#(1)$$

where i is an aerosol diameter index, j is a bubble diameter index, and k is a grid index. Eff is aerosol deposition efficiency of single bubble. Fig. 3 shows the process that bubble goes through for a PS. As the bubble rises, it is analyzed in each cell by the three modules: bubble formation, bubble breakup and deposition velocity. SPS starts its analysis from the

bottom of the tank (z=0), as seen in Fig. 3, and simulates the bubble's movement from grid to grid (z=z+Δz), until the bubble escapes through the water surface.

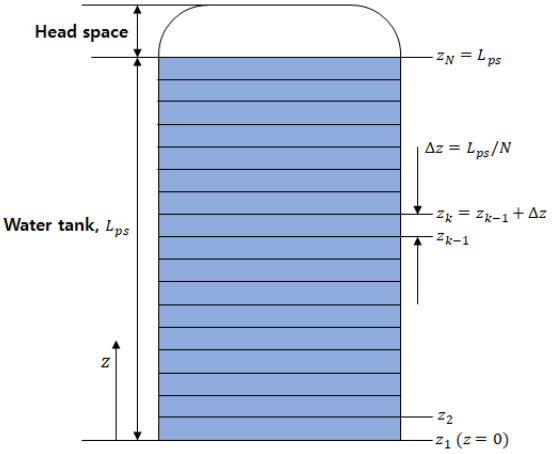

Fig. 3. Grid in a water pool

2.1. Bubble formation module

SPS's bubble formation module involves following subsequent modules: Bubble size, bubble shape.

2.1.1. Bubble size

Large size bubble is initially generated when the gas is released through the orifice. The relationships between the vent design and the bubble size is as follows:

$$\mathrm{V} = \begin{cases} 0.6731\mathrm{We}^{0.73}\mathrm{Eo}^{0.73}\mathrm{D}^{3} & \#\text{horizontal} \\ 0.0673\mathrm{We}^{0.46}\mathrm{Eo}^{-0.5}\mathrm{D}^{3} & \#\text{downcomer} \\ 2.7097\mathrm{We}^{0.46}\mathrm{Eo}^{-0.5}\mathrm{D}^{3} & \#\text{quencher} \end{cases} \#(2)$$

2.1.2. Bubble shape

The shape of bubbles can be calculated by the work of Paul's model [1].

2.2. Bubble breakup module

The BUSCA and SPARC codes assume that a single representative sized bubble is generated by the orifice. BUSCA assumes the aerodynamic mass mean diameter (AMMD) of daughter bubble is 5.62mm regardless of pool and gas conditions. On the other hand, SPARC assumed that the diameter of representative bubble is linearly decreases regardless of environmental conditions. Consequently, both bubble breakup models are too simplistic.

Hence, our code uses more realistic breakup model developed by Martinez-Bazans [2, 3]. Expressing a daughter bubble's probability density function as a function of dimensionless diameter is presented as follows:

$$f^*(d^*_{d,b1}) = \frac{\left[d^{*\frac{2}{3}}_{d,b1} - \Lambda^{\frac{5}{3}}\right]\left[\left(\frac{1}{2}\left(1 - d^{*3}_{d,b1}\right)\right)^{\frac{2}{9}} - \Lambda^{\frac{5}{3}}\right]^2}{\int_{d^*_{min}}^{d^*_{max}} \left[d^{*\frac{2}{3}}_{d,b1} - \Lambda^{\frac{5}{3}}\right]\left[\left(\frac{1}{2}\left(1 - d^{*3}_{d,b1}\right)\right)^{\frac{2}{9}} - \Lambda^{\frac{5}{3}}\right]^2 d(d^*_{d,b1})} \#$$

… … (3)

where $\Lambda^{5/3} = (12\sigma/\rho_l)\epsilon^{-2/3}d_{m,b}^{-5/3}$. Then the maximum dimensionless bubble diameter d^*_{max} can be expressed as Eq. (4).

$$d^*_{max} = \frac{\left[d^3_{m,b} - 2\left(\frac{12\sigma}{\beta\rho_l d_{m,b}}\right)^{\frac{9}{2}}\epsilon^{-3}\right]^{\frac{1}{3}}}{d_{m,b}} \#(4)$$

2.3. Deposition velocity module

Gas freely circulates in a bubble, relative fluid velocity is formed between the surrounding water and circulating gas. Inner gas circulation is graphically describable as Fig. 4. The net local deposition velocity (v_{net}) can be defined by the vector sum of all deposition velocity terms: centrifugal deposition velocity (v_c), thermophoresis velocity (v_{th}), Brownian diffusion velocity (v_B), and gravitational depositional velocity (v_{grav}), as shown in following equation:

$$v_{net} = v_c + v_{th} + v_B + v_{\mathrm{grav}}\cos\beta \#(5)$$

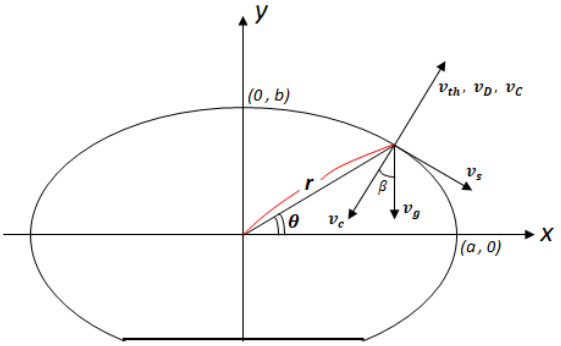

Fig. 4. Scheme of projected bubble

SPS uses the definitions from BUSCA for following deposition velocity: Thermophoresis velocity, gravitational depositional velocity. SPS uses Brownian diffusion velocity of SPARC model. Centrifugal deposition velocity can be described as Eq. (6).

$$v_c = v_s^2 v_{\mathrm{grav}}/r_b g \#(6)$$

where v_s is tangential circulation velocity as shown in Eq. (7), where $\sinh\varphi = (a/b)^2 - 1$, and $\cosh\varphi = 1 - (b/a)^2$.

$$v_s = \frac{0.5 v_r \left(\frac{r_b \sin\theta}{a}\right)}{[\sinh\varphi - \cosh^2\varphi \cot^{-1}\sinh\varphi]\sqrt{\left(\frac{r_b \cos\theta}{b}\right)^2 + \sinh^2\varphi}} \# \quad \ldots\ldots (7)$$

Since Kota Fujiwara reported MELCOR's tangential circulation velocity is nearly twice larger than experiment data, Eq. (7) is derived by multiplying adjusting coefficient 0.5 to the MELCOR's tangential circulation velocity.

SPS used Jamialahmadi's bubble rise velocity model because it shows very close results to the experimental data and it is well validated as well (see Eq. (8)).

$$v_r = \frac{-v_{sp} v_w}{\sqrt{v_{sp}^2 + v_w^2}} \#(8)$$

where

$$v_w = \sqrt{\frac{2\sigma}{2r_b(\rho_l + \rho_g)} + g r_b} \#(9)$$

$$v_{sp} = \frac{\frac{4(\rho_g - \rho_l) g r_b^2}{18\mu_l}(3\mu_l + 3\mu_g)}{(2\mu_l + 3\mu_g)} \#(10)$$

2.4. Deposition at jet injection site

This study involves three subsequent deposition models for deposition near jet injection site: Vent exit centrifugal deposition, diffusional deposition, and impaction. These specific models are benchmarked from SPARC.

3. Validation

There are several PS experiment studies to assess the deposition efficiency. Selected experiment pieces are limited to those that did not contain a high steam fraction in the gaseous phase, because high steam gaseous experiments show very unstable DFs. Therefore, PS experiment programs such as RCA and POSEIDON were used to validate our code.

Since SPARC shows much more reasonably close DFs than BUSCA, we are going to validate our code DFs by comparing experimental DFs, and DFs simulated by SPARC. For the more intuitive analysis, we defined the deviation as follows:

$$\text{Deviation} = \left|\frac{\text{DF}_{\text{code}} - \text{DF}_{\text{exp,mean}}}{\text{DF}_{\text{exp,mean}}}\right| \times 100\% \#(11)$$

Each experiment conditions are summarized in Table 1-1 and 1-2.

Table 1-1. RCA experiment conditions

Program	RCA1	RCA2	RCA3	RCA4
Pressure (bar)	2.80	2.80	2.80	2.80
Gas temperature (℃)	120	120	120	120
Flowrate (g/s)	7.20	7.20	7.20	7.20
Steam fraction	0.00	0.00	0.00	0.00
Mean diameter (μm)	3.25	4.02	3.46	4.03
Water temperature (℃)	120	120	120	120
Tank depth (m)	0.25	0.50	1.25	2.50

Table 1-2. POSEIDON experiment conditions

Program	PA10	PA11	PA12	PA13
Gas temperature (℃)	222	256	237	270
Flowrate (g/s)	38.33	38.33	34.72	34.72
Steam fraction	0.04	0.04	0.00	0.00
Mean diameter (μm)	0.3	0.3	0.3	0.3
Water temperature (℃)	80	75	72	63
Tank depth (m)	4.00	2.00	1.00	0.30

Following figures show DF comparisons (see Fig. 5 and Fig. 6).

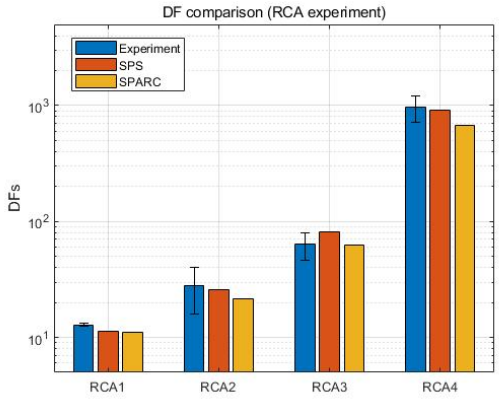

Fig. 5. DF comparison (RCA)

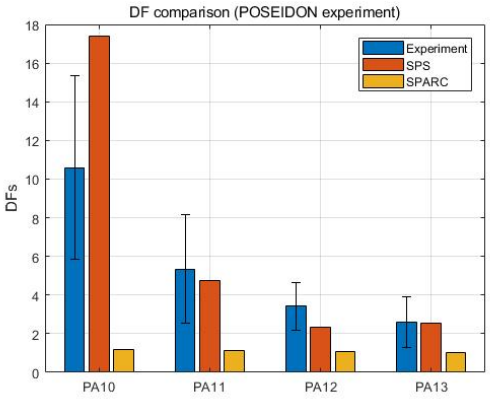

Fig. 6. DF comparison (POSEIDON)

The ranges of DFs found in the experiments are identified by the black barkers. RCA studied larger particle removal and POSEIDON studied for smaller particle removal. Following figures show deviation comparison (see Fig. 7 and Fig. 8).

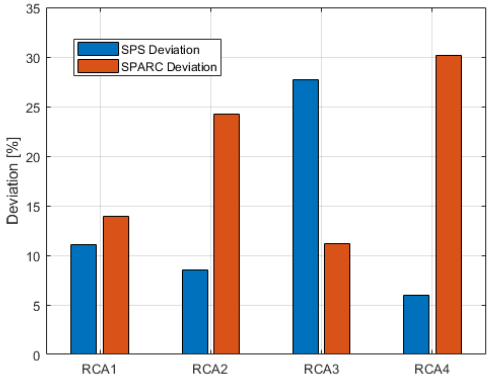

Fig. 7. Deviation comparison (RCA)

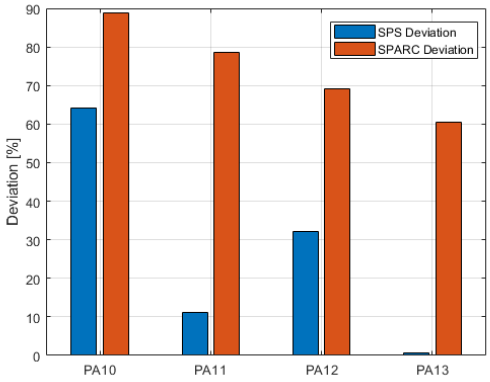

Fig. 8. Deviation comparison (POSEIDON)

4. Conclusion

For the more precise pool scrubber's DF prediction, some improvements are involved in newly developed PS code (SPS code) in this study. More realistic bubble breakup model and hydrodynamic models are involved. Achieved DFs are compared to the DFs obtained by experiments and SPARC code. Consequently, SPS shows lower deviation than SPARC except RCA2 experiment setup. Hence, we can conclude that SPS shows better DF prediction than existing codes (BUSCA and SPARC). However, since the number of experimental DFs are limited in this study, more PS experiments are needed for the more precise validation.

Nomenclature

a : Major axis length
b : Minor axis length
d, D : Diameter
g : Gravitational acceleration
r : Radius
We : Weber number
Eo : Eotvos number
V : Volume
μ : Viscosity
ρ : Density
σ : Surface tension

Subscription

m : Mother
b : Bubble
d : Daughter
g : Gas
l : Liquid

Acknowledgement

This research was supported by National Nuclear R&D Program (Human Resources Program in Energy Technology) through the National Research Foundation of Korea (NRF) by the Ministry of Science, Science and Technology (NRF-2018M2C7A1A02071198)

Reference

[1] Paul, D. D., et al. Radionuclide scrubbing in water pools-gas-liquid hydrodynamics. No. EPRI-NP--4113-SR. 1985.
[2] Martinez-Bazan, C., J. L. Montanes, and Juan C. Lasheras. "On the breakup of an air bubble injected into a fully developed turbulent flow. Part 1. Breakup frequency." Journal of Fluid Mechanics 401 (1999): 157-182.
[3] Martinez-Bazan, C., J. L. Montanes, and Juan C. Lasheras. "On the breakup of an air bubble injected into a fully developed turbulent flow. Part 2. Size PDF of the resulting daughter bubbles." Journal of Fluid Mechanics 401 (1999): 183-207.
[4] Fujiwara, Kota, et al. "Experimental study of single-bubble behavior containing aerosol during pool scrubbing." Nuclear Engineering and Design 348 (2019): 159-168.
[6] Owczarski, P. C., and K. W. Burk. SPARC-90: A code for calculating fission product capture in suppression pools. No. NUREG/CR-5765; PNL-7723. Nuclear Regulatory Commission, Washington, DC (United States). Div. of Regulatory Applications; Pacific Northwest Lab., Richland, WA (United States), 1991.
[7] Ramsdale, Susan A., Salih Güntay, and Hans-Günter Friederichs. BUSCA-JUN91 reference manual. No. PSI--95-05. Paul Scherrer Inst.(PSI), 1995.